Soils and Rocks
www.soilsandrocks.com
An International Journal of Geotechnical and Geoenvironmental Engineering
ISSN 1980-9743
ISSN-e 2675-5475

Application of artificial neural networks in predicting the Mohr-Coulomb shear strength parameters

Francisco de Assis Linhares Fernandes Filho[1#], Silvrano Adonias Dantas Neto[1], Daniel Gurgel do Amaral Mota[1]

Article

Keywords
Artificial neural networks
Cohesion
Friction angle
Machine learning
Multilayer perceptrons

Abstract

The determination of soil shear strength parameters is essential in geotechnical projects and traditionally relies on laboratory tests, which can be expensive, time-consuming, and, in some cases, unfeasible. As a preliminary alternative, correlations based on in-situ tests can be used, however, such correlations are generally limited to sands or clays, restricting their applicability in many practical situations. A potentially more comprehensive solution is the development of models capable of relating the Standard Penetration Test (SPT), the most widely used field test in geotechnical practice, to the Mohr-Coulomb strength parameters, cohesion (c') and friction angle (ϕ'), while accounting for different grain-size fractions. This task is challenging due to the high variability of the variables involved, however, by using machine learning techniques, such as artificial neural networks, which are capable of handling complex and nonlinear relationships, it has been possible to overcome part of these limitations. The proposed model also incorporates a relevant contribution: the numerical treatment of the "soil type" variable, allowing the network to account for differences among sandy, silty, and clayey soils. With a representative dataset, the model achieved correlation coefficients of 0.85 (training) and 0.90 (testing), with mean errors of 5.3 kPa for c' when $c' < 20$ kPa, and 2.36° for ϕ' in the range $25° \leq \phi' < 35°$. In addition to demonstrating superior performance compared to models available in the literature, the model is capable of handling different grain-size fractions. It is concluded that the model shows satisfactory performance for preliminary applications in geotechnical engineering practice, allowing estimates of the strength parameters within well-defined validity ranges, however, it does not replace the need for laboratory testing.

1. Introduction

In geotechnics, the Mohr-Coulomb model is commonly used to represent soil shear strength, with cohesion and friction angle as key parameters. These parameters are obtained under drained (effective stress) or undrained (total stress) conditions. The model is widely used because its parameters are easy to understand based on the soil's physical and structural characteristics and can be derived from relatively simple lab tests (Labuz & Zang, 2012).

The Mohr-Coulomb constitutive model is applied in many analytical methods for geotechnical projects, including slope stability analysis and elastoplastic stress-deformation studies (Xiang & Zi-Hang, 2017; Amouzou & Soulaimani, 2021). Its parameters can be derived from lab tests, such as direct shear and triaxial tests, or from correlations with results of field tests like the SPT and CPT. While lab tests allow for specific adjustments, they depend on sample quality and are time-consuming. Thus, correlations are often used to predict cohesion and friction angles, complementing lab tests and reducing costs and investigation time.

Correlations, particularly for predicting the internal friction angle of granular soils (sands), or the undrained strength of fine soils (clays), often use the number of blows in the SPT test (N_{SPT}), due to the wide use of this field test around the world (AbuSerriya & Osman, 2023). Therefore, it is observed that the existing correlations cannot be used for predicting the effective cohesion and the internal friction angle of other types of soils, such as, clayey soils, silty soils, and sandy soils.

Recently, the application of Machine Learning techniques, such as artificial neural networks (ANN) and hybrid neural models, has expanded significantly within geotechnical engineering, largely due to their capacity to handle nonlinear and complex soil-structure relationships (Alanis et al., 2019; Dolatshahi & Molladavoodi, 2024;

#Corresponding author. E-mail address: assis_linhares@hotmail.com
[1]Universidade Federal do Ceará, Departamento de Engenharia Hidráulica e Ambiental, Fortaleza, CE, Brasil.

Submitted on November 7, 2024; Final Acceptance on January 27, 2026; Discussion open until November 30, 2026.

Editor: Renato P. Cunha

https://doi.org/10.28927/SR.2026.009124

Dowlatshahi et al., 2023). Their use has been demonstrated in a wide range of studies, including the prediction of undrained shear strength in sensitive clays (Elsawy et al., 2022), the back-analysis of rock and tunnel parameters through Gaussian Process models combined with optimization algorithms (Zheng et al., 2022; Zhan et al., 2023), and the estimation of rock elastic modulus using hybrid Random Forest methods (Li & Dias, 2023). Additional works have investigated soil classification using CPT data (Chala & Ray, 2023b), ground-subsidence risk in urban environments (Lee et al., 2023), and the prediction of dynamic soil properties such as the damping ratio (Lendo-Siwicka et al., 2023). Advanced applications have also emerged, such as predicting the bearing capacity of foundations using convolutional neural networks (Cheng et al., 2023), estimating shear-wave velocity (Chala & Ray, 2023a), analyzing rocking-foundation behavior under seismic loading (Gajan, 2023), optimizing shield-tunneling advance rates through LSTM-based models (Yang et al., 2024), and forecasting utility-tunnel performance in soft soils using deep learning (Gao et al., 2024).

Within this broader context, the present manuscript introduces an ANN-based predictive model, specifically a Multilayer Perceptron (MLP), designed to estimate the effective cohesion and internal friction angle of soils. The model relies on variables derived from the Standard Penetration Test (SPT), which remains one of the most widely used in-situ investigation methods in geotechnical practice in Brazil and internationally.

2. Artificial neural networks

2.1 Generalities

Artificial Neural Networks (ANN) are popular machine learning techniques that simulate the learning mechanisms of biological organisms (Janiesch et al., 2021). The human nervous system contains cells called neurons. The neurons are connected to each other by axons and dendrites, and the connection regions between axons and dendrites are called synapses. The forces of synaptic connections often change in response to external stimuli. This change is like learning in living organisms.

McCulloch & Pitts (1943) presented the artificial neuron (Figure 1) as an analogy to the biological neuron. Each artificial neuron is characterized by three main components: one set of input signals $\boldsymbol{x}=[x_1, x_2, \ldots, x_m]^T$; the vector of synaptic weights $\boldsymbol{w_k}=[w_{k1}, w_{k2}, \ldots, w_{km}]^T$; and the induced local field (v_k) in the k^{th} artificial neuron, calculated from the sum of the linear combination of the weighted input signals (Equation 1).

$$v_k = \sum_{j=1}^{m} w_{kj} x_j + b_k \tag{1}$$

Where b_k is the bias in the k^{th} artificial neuron, and $f(\cdot)$ is the activation function that determines the output of the k^{th} neuron (y_k) (Equation 2 and 3).

$$y_k = f(v_k) \tag{2}$$

$$y_k = f\left(\sum_{j=1}^{m} w_{kj} x_j + b_k\right) \tag{3}$$

The activation function $f(v_k)$ played a key role in introducing nonlinearities in artificial neurons. The choice of activation function is crucial since it directly influences the capacity of the ANN to learn and generalize complex patterns in the input data. Common functions include the sigmoid, hyperbolic tangent, ReLU (Rectified Linear Unit), and others, each offering unique characteristics of non-linear behavior that impact the efficiency of the training and capacity to represent the network (Parhi & Nowak, 2020).

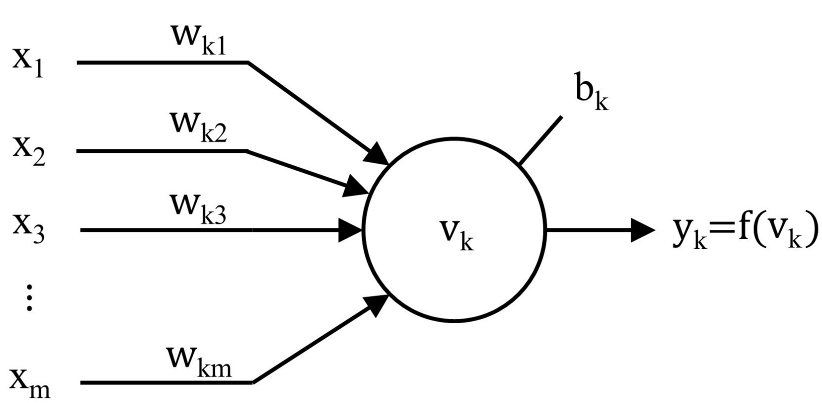

Figure 1. Artificial Neuron (modified from Haykin, 2009).

2.2 Multilayer perceptrons

The multilayer perceptron (MLP) represents an important class of ANN used to model complex, multivariate, and non-linear phenomena. This is a feedforward neural network consisting of three types of layers: input layer, consisting of nodes that receive external signals, one or more hidden neuron layers, responsible for increasing the input capacity of ANN to extract the more complex behavior of the modeled phenomenon and the output layer, consisting of neurons whose signals represent the response to the external signal presented to the ANN (Haykin, 2009).

One of the most important properties of an ANN is its capacity to learn with the environment in which it operates and improve its performance using an ongoing training process. The training of an ANN consists of altering all synaptic weights and biases from the known experience of the studied phenomenon, generally available in a set of in-out data known as a learning set. Usually, the adjust of synaptic weights and bias (training) of a multilayer perceptron is performed by the Backpropagation Algorithm developed by Rumelhart et al. (1986).

After training, the capacity of generalization of the network is assessed using a set of data, known as test set, consisting of values not used during the training. The generalization capacity refers to the skill of the network to satisfactorily predict the parameters of interest from input data different from those present in the training set. A good capacity to generalize is essential to ensure that the ANN can represent the knowledge on the modeled phenomenon, instead of only memorizing the existing data in the training set (Zhang et al., 2021).

2.3 ANN applications in geotechnical engineering

Artificial Neural Networks (ANN) have been highlighted in geotechnical engineering, several studies have fulfilled their potential, ranging from the prediction of soil properties to the analysis of the mechanical behavior of geotechnical structures.

Ray et al. (2021), Millán et al. (2021) and Sethy et al. (2021) explored the use of ANN to predict shallow foundation bearing capacity. Khatti & Grover (2022), Boadu et al. (2013), Mohammadi et al. (2022) and Bahmed et al. (2019) applied ANN to predict soil properties. Aouadj & Bouafia (2022), Moayedi & Hayati (2018), and Díaz et al. (2018) focused on using ANN to estimate settlements and other responses of geotechnical structures, evidencing the capacity of the networks to learn non-linear patterns from historical data.

Nejad & Jaksa (2017), Liu et al. (2020) and Dantas Neto et al. (2014) concentrated their studies to predict behaviors of piles, evidencing the ANN capacity of modelling complex non-linear relations between historic data and pile behavior.

Lin et al. (2022), Iyeke et al. (2016), Abu-Farsakh & Mojumder (2020) and Zhang et al. (2022) applied artificial neural networks (ANN) to predict the soil shear strength, demonstrating the capacity of such networks to model the relation between physical soil characteristics and their mechanical properties.

Moayedi et al. (2020), Benali et al. (2021), Goudjil & Arabet (2021) and Alzo'Ubi & Ibrahim (2021) used ANN to predict pile behavior under different types of soil and bearing conditions. Gupta et al. (2022), Meng et al. (2021) and Paliwal et al. (2022) employed ANN to assess slope stability, showing the effectiveness of the networks when analyzing factors that influence slope stability.

3. Materials and methods

3.1 Defining input variables of the ANN model

To build and implement the proposed model, in order to use variables that could represent the soil shear strength in situations in which the extraction of undisturbed samples to perform laboratory tests is unfeasible, the input variables chosen for the ANN are:

- N_{SPT}: number of blown in the SPT.
- σ'_v: effective vertical stress, in kPa.
- Soil type: considered sandy, clayey, and silty soils.

The use of N_{SPT} as an input variable in the neuronal model to estimate soil strength parameters is justifiable due to its widespread application and frequent use in geotechnical investigations, especially in Brazil. The standard penetration test (SPT) is commonly adopted due to its low cost and simplicity in providing data on soil properties. However, it is important to consider some limitations regarding the use of N_{SPT} values, such as the influence of energy applied on the sampler during the test and the sampling conditions, which may affect the accuracy of the results. Moreover, the N_{SPT} may be unable to properly capture the variations in the soil strength under different humidity and compaction conditions, which could restrict their accuracy in some geotechnical applications (Schmertmann & Palacios, 1979).

The effective vertical stress (σ'_v) was selected as an input variable because it is the parameter representing the influence of the stress state in the soil shear strength (Lambe & Whitman, 1979). It can also be determined from basic data, such as knowing the apparent specific weights of the materials.

The input variable of the ANN model named as "soils type" is used to take into account the differences of shear strength parameters of sandy, clayey, and silty soils. According to the Mohr-Coulomb criterion, the shear strength of the soils is governed by a cohesive component, characteristic of fine soils, and another frictional, which is quite notorious in granular soils, evidencing the influence of the soil type in predicting its strength parameters. The soil type in the proposed model is classified according to the most predominant fraction. Therefore, soils such as sandy clays and silty clays are considered clayey soils. Likewise, clayey sands and silty sands are classified as sandy soils, and sandy silts and clayey silts are considered silty soils.

Therefore, it may be considered that the proposed neuronal model takes into consideration a greater variety of soil types compared to those used to predict cohesion and friction parameters based on corrections from the literature (AbuSerriya & Osman, 2023).

3.2 Data collection and normalization of the variables

The database used to train and test the ANN model to predict the effective strength parameters of the soil is based on 168 results of consolidated undrained (CU) and consolidated drained (CD) triaxial tests and direct shear tests in the studies by AbdelSalam et al. (2014), Souza (2014), Camelo et al. (2017), Carvalho (1991), Coutinho et al. (2000), Dias (1987), Gomes (2003), Gon (2011), Lafayette (2006), Lima (2002), Magalhães (2013), Marques (2006), Moraes (2010), Peixoto (2001), Pérez (2014), Ribeiro et al. (2012), Santana (2016), Santos (2007), Silva (2007), Souza (2012) and Suzuki (2004). The complete list of these data is presented in Table A1 in Appendix A. Figures 2 and 3 below show the bar charts of the input and output variables used in the model.

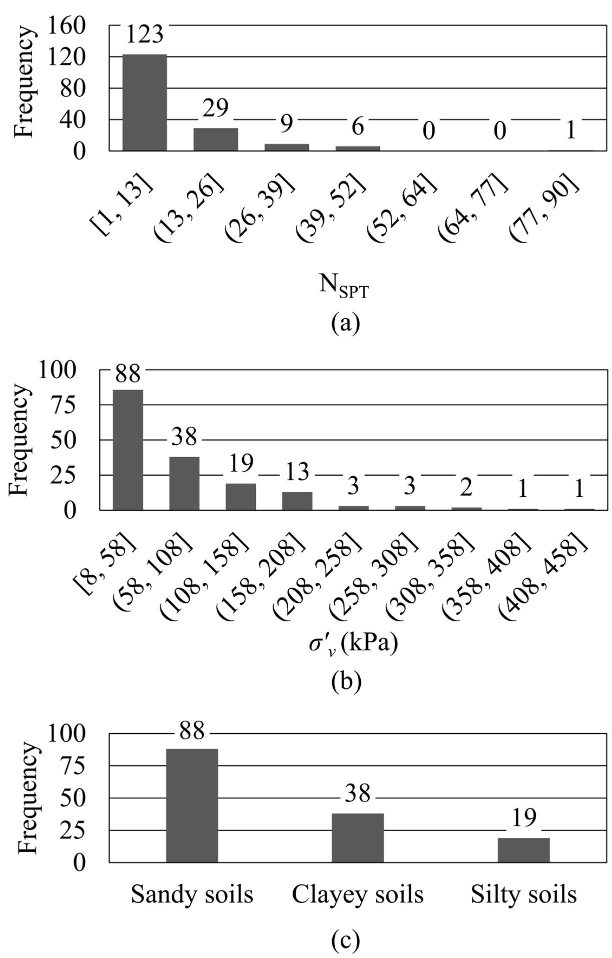

Figure 2. Bar chart input variables (a) N_{SPT}, (b) σ'_v and (c) Soil type.

To do so, bearing in mind that the domain of the function is contained between the 0 and 1 limits, the input and output ANN data were normalized between values 0.15 and 0.85 according to Equation 4.

$$\frac{x_{norm} - x_{norm,min}}{x_{norm,max} - x_{norm,min}} = \frac{x - x_{min}}{x_{max} - x_{min}} \tag{4}$$

To incorporate the soil type into the machine learning model, this categorical variable was converted into a numerical scale (sand = 0.15, clay = 0.50, silt = 0.85). This encoding allowed the variable to be treated consistently with the other inputs. The statistical relationships among the input variables can be evaluated using the correlation matrix presented in Figure 4, which N_{SPT} shows strong association with soil type, reflecting the tendency of sandy soils to exhibit higher penetration resistance compared to fine materials.

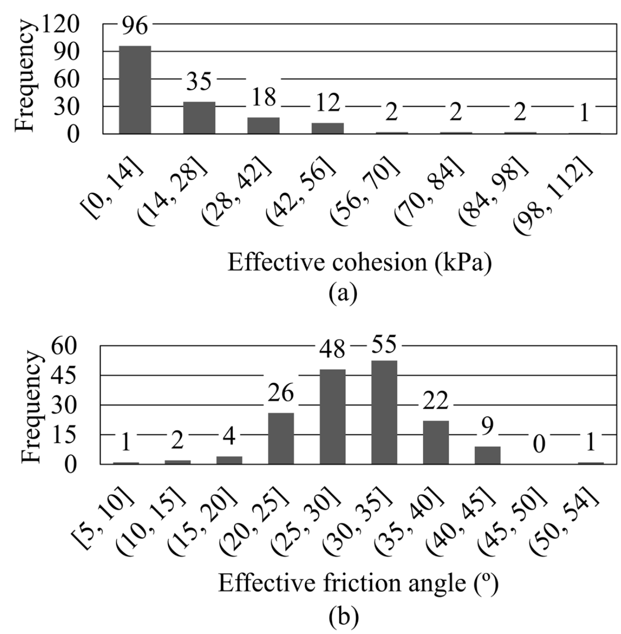

Figure 3. Bar chart output variables (a) c' and (b) ϕ'.

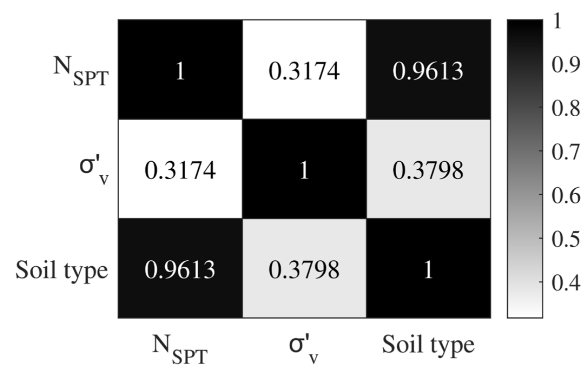

Figure 4. Correlation Matrix of Input Variables.

Additionally, the moderate correlations involving σ'_v indicate that increases in effective vertical stress also contribute to greater soil stiffness.

3.3 Training, testing, and validation of ANN

Although more advanced machine learning techniques, such as XGBoost and CatBoost, as well as more practical hybrid approaches that combine multiple linear regression with artificial neural networks, are available, multilayer perceptrons were adopted because they directly meet the objective of this study. They are capable of representing the nonlinear relationships between N_{SPT}, effective stresses, and the parameters c' and ϕ', while also allowing the generation of practical design charts. Furthermore, this type of model is widely used in geotechnical literature, facilitating comparison with previous studies.

For the development of an ANN with good generalization capacity in predicting the soil strength parameters, a number of network architectures were tested. The networks were then trained, tested and validated based on the database collected. For the ANN concept, the sigmoid activation function was used, presented in Equation 4, which provides more stability during the network learning.

$$f\left(v_k\right) = \frac{1}{\left(1+e^{-v_k}\right)} \tag{5}$$

No stratification by soil type and no formal outlier detection procedure were applied during the train-test-validation split. The data were randomly partitioned, following the methodology of Dantas Neto et al. (2017) and Tizpa et al. (2015), into training (85%) and testing (15%) subsets, with an additional 38 samples reserved for validation. The objective was to evaluate the overall predictive capability of the model across the entire data range, and this choice is further justified by the relatively small number of samples in each soil category, which could lead to excessively reduced subsets if stratification were applied.

The network's generalization capacity was rigorously tested, focusing on preventing overfitting, which was monitored through cost function variations, particularly the root-mean-square (*RMS*) error.

The choice of the ANN architecture considered satisfactory was made by tracking the point at which cost function values began to rise during testing, indicating the onset of memorization rather than generalization. Performance was further validated by testing the ANN with previously unseen input combinations, confirming its predictive robustness. Training and testing were conducted using QNET2000 software with standard configurations and monitored learning rates and momentum parameters, as recommended by Dantas Neto et al. (2017). Model efficacy was assessed through correlation coefficients and *RMS* error metrics, affirming the model's accuracy in generalizing input-output relationships in the dataset.

4. Results and discussions

4.1 Defining the ANN model architecture

The synapses and biases of all tested models were optimized with up to 500,000 epochs, since these are considered sufficient to define the convergence of the training algorithm of the start of overtraining, characterized by a drop in the *RMS* error during training stage and a rise in the *RMS* error at the testing stage.

Figure 5 shows the learning curves in relation to the correlation coefficient and *RMS* error for the training and testing stages of the models, where an A-*X*–*Y*–*Z* is a code that represents an ANN model consisting of an input layer with *X* neurons, a hidden layer with *Y* neurons and an output layer with *Z* neurons. Note that the shape of the correlation curves seems to be the inverse of the *RMS* curves, indicating that both parameters can be used to express the convergence of the learning algorithm.

The number of iterations used to define the optimum network of each investigated architecture is defined by the following criteria: convergence of the learning algorithm that occurs when the correlation curves become asymptotic during the test and training stages, or when the *RMS* error calculated during the test phase increases, thereby characterizing overtraining. When the learning curves expressed by the *RMS* error variation against the number of iterations are analyzed, overtraining is not expected in all tested model architectures, since there is no increase in the *RMS* values at the testing stage.

Bearing this in mind, an analysis of Figure 5 could show that the increase in correlations with the iterations during the training is observed only for some tested ANN. It is also worth mentioning that considering the results obtained in the training phase, the convergence of the most tested ANN models occurred after 500,000 iterations. However, the networks A:3-5-2 and A:3-5-3-2 had overtraining, since there was an increase in the *RMS* in the correlation from a certain number of seasons (Haykin, 2009).

Table 1 then presents the architecture and number of iterations considered optimized for each ANN, and it is noticeable that all networks showed a similar efficiency. However, the ANN defined by the A:3-5-3-2 provided the best results, with the highest correlation values during both phases with a lower number of iterations, being thereby selected as the model for predicting the soil strength parameters.

The validation process was then performed for network A:3-5-3-2 in order to assess the quality of the response to unknown data by the network. The results obtained were plotted in the dispersion graphs shown in Figure 6, in which it can be noted that the proposed model was unable to reproduce satisfactorily the behavior of the soils throughout the interval that comprises the validation data.

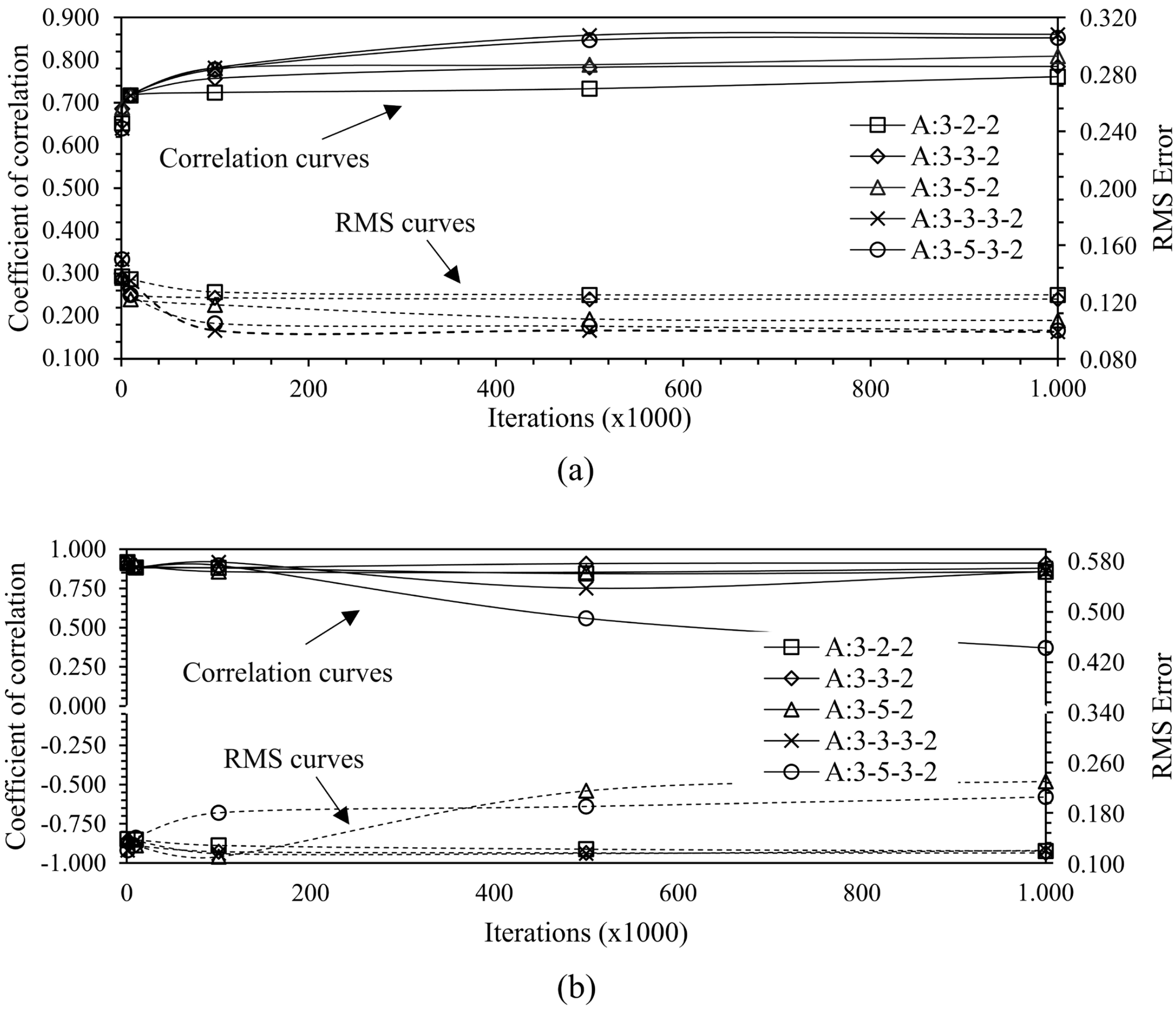

Figure 5. *RMS* history and correlations x iterations for ANN models on *c'* and ϕ' prediction: (a) training and (b) testing.

Table 1. Correlations and number of Iterations for optimized ANNs.

Architecture	Coefficient of correlation		Iterations at convergence
	Training	Test	
A: 3-2-2	0.73	0.85	500,000
A: 3-3-2	0.78	0.91	500,000
A: 3-5-2	0.79	0.85	500,000
A: 3-3-3-2	0.78	0.92	100,000
A: 3-5-3-2	0.85	0.90	100,000

When predicting cohesion, it was found that the neural network was unable to predict values of more than 20 kPa, achieving a mean error ($\bar{e}$) of 22.8 kPa for *c'* outside this band. However, within the acceptable interval, (*c'* < 20 kPa) it was found that $\bar{e}$ = 5.3 kPa, considered reasonable for a prediction model prepared from simple variables. The model's confidence was then calculated with the validation set, taking into consideration that the error distribution is approximately normal. The results in Table 2 show that, despite the occurrence of high errors, there is a 72% confidence that the mean of errors of a group of samples with strength parameters estimated by the proposed ANN will be $\bar{e}$ = 5 kPa.

In turn, the ANN prediction of the friction angle could be considered satisfactory within an interval 25°≤ ϕ' <35°, where the mean calculated error was 2.36º. For values outside this band, the errors found were much higher as seen in Figure 6 (b), although Table 2 shows that the confidence of the model for ϕ' has been higher in relation to the *c'* calculation.

Table 2. Confidence of model in *c'* and ϕ' predictions.

c'		ϕ'	
Error (kPa)	**Confidence**	**Error (o)**	**Confidence**
+2	0.73	0.85	73%
+3	0.78	0.91	77%
+4	0.79	0.85	81%
+5	0.78	0.92	85%
+6	0.85	0.90	89%

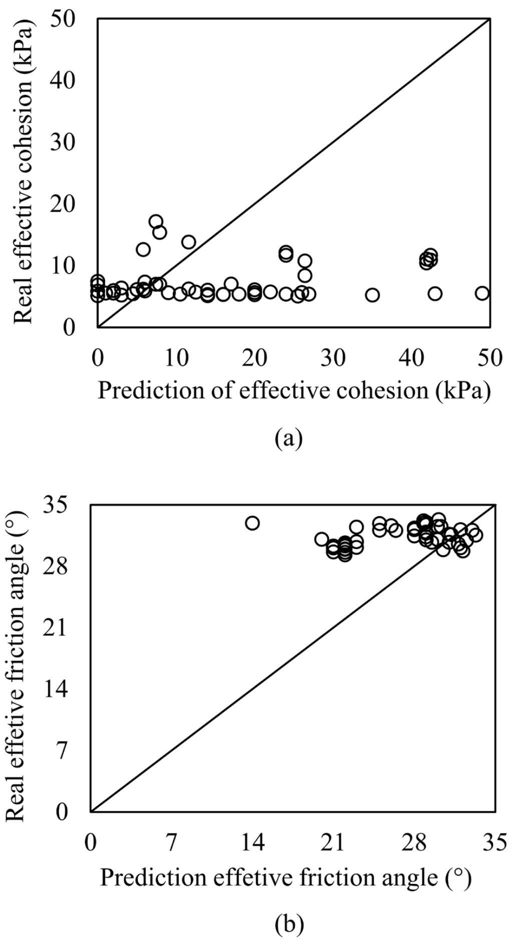

Figure 6. Actual vs. measured values during validation for A:3-5-3-2 in the prediction of: (a) *c'* and (b) ϕ*'*.

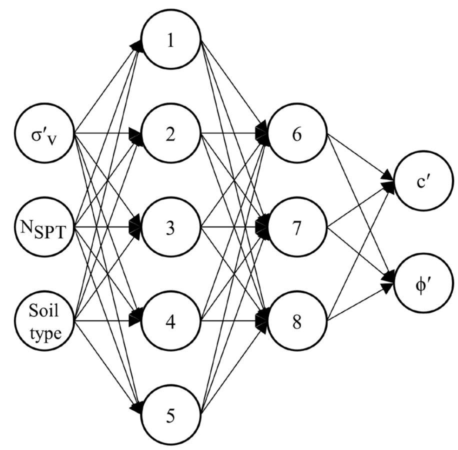

Figure 7. RNA A:3-5-3-2 architecture.

Such limitations of the proposed ANN reflect the constitution of the database, which has 75% of the data used for training and validation with cohesion less than 14 kPa and 73% with 25º ≤ ϕ' ≤ 35º, unlike the expected generalization behavior (Dantas Neto et al., 2017). Thus, the proposed neural network is unable to capture fully the mechanical behavior of the soils from the input variables, while the use of the model can be effective in running the solution feasibility study for an intervention or preliminary design. In any case, however, do not discard the need to undertake laboratory tests to obtain the soil strength parameters.

The modeling results also showed that the prediction of ϕ*'* for clay soils failed. This fact may be a result of not considering the less abundant soil fractions, since the frictional part of the shear strength is closely linked to the granular fraction (Lambe & Whitman, 1979) and the proposed ANN used as an input in a simplified classification of the soil type, in which the possible inputs are clay, silt and sand. This is also observed when the Input Node Interrogator (NI), obtained by QNET2000 for the soil type variable, is analyzed, which evidences the lowest dependence for this input. However, the NI results for the model validate the use of the chosen input variables, since the proportions are balanced. Prediction *c'* shows NI (σ_v*'*) = 30.38%, NI (N_{SPT}) = 59.17% and NI (soil type) = 10.46%, differing from ϕ', which presented NI (σ_v*'*) = 35.89%, NI (N_{SPT}) = 52.64% and NI (soil type) = 11.47%.

4.2 Presentation of the ANN model

The previous ANN analysis resulted in the choice of the A:3-5-3-2 network architecture with convergence in 100,000 iterations and use of the sigmoid activation function, in which the correlation coefficients were obtained for the training and testing stages equal to 0.85 ad 0.90, respectively. The resulting architecture can be verified in Figure 7, in which the input parameters and neurons are illustrated by interconnected circles with the adjacent layers, with no connection between the same layer's processor units.

Table 3. Synaptic weights and bias for the first hidden layer.

Inputs	1	2	3	4	5
x1	-1.179	-1.657	-0.787	-7.350	-3.917
x2	-0.539	-2.276	4.865	0.804	0.754
x3	-0.871	6.382	-3.481	2.479	-0.219
bias	0.794	1.553	-1.950	-2.239	3.766

Table 4. Synaptic weights and bias for the second hidden layer.

Inputs	1	2	3
x1	-0.152	-1.785	-0.428
x2	3.085	0.143	-3.784
x3	-2.793	-0.757	-5.791
x4	1.738	3.574	-2.951
x5	1.118	-1.511	5.773
bias	-0.734	1.553	0.162

Table 5. Synaptic weights and bias for output layer.

Inputs	1	2
x1	1.154	-4.490
x2	2.283	2.956
x3	-6.201	4.757
bias	2.427	0.611

The synaptic and bias of each neuron can be seen in Tables 3, 4 and 5, and it is worth mentioning that the neural networks are fairly sensitive alterations in those values and, consequently, must be used down to the last significant algorithm.

Based on the results obtained by ANN A:3-5-3-2, c' and ϕ' values were then generated for each soil type considering different ordered pairs, in which N_{SPT} varied from 2 to 50 blows and σ'_v varied from 20 to 200 kPa. With that, the abacus shown in Figure 8 was generated, where each graph includes lines representing specific values of effective vertical stress, calculating the N_{SPT} and σ'_v inputs.

5. Conclusions

This article provided a neuronal model to predict the Mohr-Coulomb soil shear strength parameters, defined in effective stress terms (drained parameters), having as input variables σ'_v, N_{SPT}, and soil type. After analyzing different architectures, the chosen model presented the best performance with network architecture A:3-5-3-2, trained for 500,000 iterations using the sigmoid activation function. This model obtained correlations equal to 0.85 and 0.90 for the training and test stages, respectively. The assessment of the residuals obtained in the test phase allowed the authors to define, with a 72% degree of confidence, that the values of the effective cohesion were situated at ±8º around the calculated value for a confidence level of 85%.

Nevertheless, attention must be given to the limitations of the model, which should be applied within the ranges of $c' \leq 20$ kPa and $25° \leq \phi' \leq 35°$, where the network exhibits better generalization capacity. Furthermore, the estimation of c' and ϕ' should be restricted to preliminary geotechnical assessments, without replacing laboratory tests.

A comparison with other predictive models was not performed, because the proposed ANN incorporates soil type as an input variable, a fundamental aspect that is not considered in the available models in the literature, making a direct comparison methodologically inappropriate. In addition to the simplicity provided by the ANNs, several charts were also developed to facilitate the estimation of the predicted parameters, eliminating the need for complementary tools or spreadsheets.

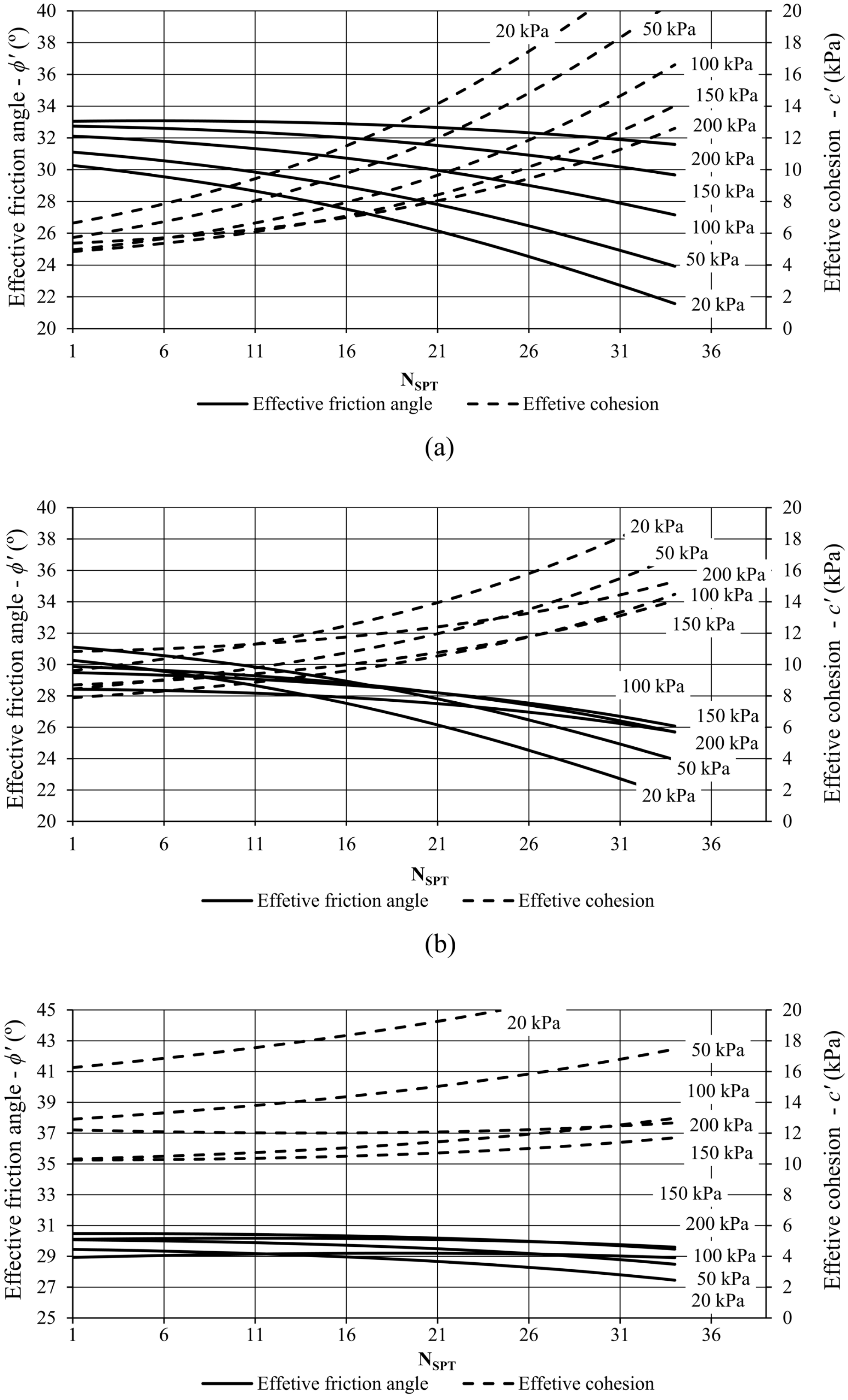

Figure 8. Abacuses with lines representing effective vertical stress for predicting soil strength parameters in: (a) sandy soils, (b) clayey soils and (c) silty soils.

Acknowledgements

The authors are appreciative of the funding support provided by Coordenação de Aperfeiçoamento de Pessoal de Nível Superior (CAPES), Universidade Federal do Ceará (UFC).

Declaration of interest

The authors have no conflicts of interest to declare. All co-authors have observed and affirmed the contents of the paper and there is no financial interest to report.

Authors' contributions

Francisco de Assis Linhares Fernandes Filho: formal analysis, validation, visualization, writing – review & editing. Silvrano Adonias Dantas Neto: conceptualization, supervision, validation, writing - review & editing. Daniel Gurgel do Amaral Mota: data curation, formal analysis, investigation, methodology, writing – original draft.

Data availability

The datasets generated analyzed in the course of the current study are available from the corresponding author upon request.

Declaration of use of generative artificial intelligence

This work was prepared without the assistance of any generative artificial intelligence (GenAI) tools or services. All aspects of the manuscript were developed solely by the authors, who take full responsibility for the content of this publication.

List of symbols and abbreviations

b	Bias
c	Cohesion (kPa)
c'	Effective cohesion (kPa)
$\bar{e}$	Mean absolute error
r	Pearson correlation coefficient
v	Induced local field
w	Synaptic weight
x	Input signals
y	Output neuron
A	ANN architecture
ANN	Artificial neural network
CD	Consolidated drained triaxial test
CPT	Cone Penetration Test
CU	Consolidated undrained triaxial test
MLP	Multilayer perceptron
NI	Node interrogator
N_{SPT}	The number of blows in the SPT test
RMS	Root-mean-square deviation
R^2	Coefficient of determination
SPT	Standard Penetration Test
X	Number of neurons in the input layer
X_{max}	Maximum values of the training database
X_{min}	Minimum values of the training database
X_{norm}	Variable after standardization
$X_{norm,max}$	Maximum limit of standardization
$X_{norm,min}$	Minimum limit of standardization
Y	Number of neurons in the hidden layer
Z	Number of neurons in the output layer
σ'_v	Effective vertical stress (kPa)
ϕ	Friction angle (º)
ϕ'	Effective friction angle (º)
$\varphi(\cdot)$	Activation function

References

AbdelSalam, S.S., Suleiman, M.T., & Sritharan, S. (2014). Modeling load-transfer behavior of H-piles using direct shear and penetration test results. *Geotechnical Testing Journal*, 37(4), 663-677. https://doi.org/10.1520/GTJ20130074.

Abu-Farsakh, M.Y., & Mojumder, M.A.H. (2020). Exploring artificial neural network to evaluate the undrained shear strength of soil from cone penetration test data. *Transportation Research Record: Journal of the Transportation Research Board*, 2674(4), 11-22. https://doi.org/10.1177/0361198120912426.

AbuSerriya, A., & Osman, B. (2023). Correlation of cohesion and friction angle based on SPT-N Values: a comprehensive review. *Journal of Civil Engineering Beyond Limits*, 4(2), 821. https://doi.org/10.36937/cebel.2023.1821.

Alanis, A.Y., Arana-Daniel, N., & López-Franco, C. (2019). *Artificial neural networks for engineering applications*. Elsevier Inc. https://doi.org/10.1016/C2018-0-01649-7.

Alzo'Ubi, A.K., & Ibrahim, F. (2021). Predicting the pile static load test using backpropagation neural network and generalized regression neural network–a comparative study. *International Journal of Geotechnical Engineering*, 15(7), 810-821. https://doi.org/10.1080/19386362.2018.1519975.

Amouzou, G.Y., & Soulaimani, A. (2021). Numerical algorithms for elastoplacity: finite elements code development and implementation of the Mohr–Coulomb Law. *Applied Sciences (Basel, Switzerland)*, 11(10), 4637. https://doi.org/10.3390/app11104637.

Aouadj, A., & Bouafia, A. (2022). CPT-based method using hybrid artificial neural network and mathematical model to predict the load-settlement behaviour of shallow foundations. *Geomechanics and Geoengineering*, 17(1), 321-333. https://doi.org/10.1080/17486025.2020.1755459.

Bahmed, I.T., Harichane, K., Ghrici, M., Boukhatem, B., Rebouh, R., & Gadouri, H. (2019). Prediction of geotechnical properties of clayey soils stabilized with lime using artificial neural networks (ANNs). *International Journal of Geotechnical Engineering*, 13(2), 191-203. https://doi.org/10.1080/19386362.2017.1329966.

Benali, A., Hachama, M., Bounif, A., Nechnech, A., & Karray, M. (2021). A TLBO-optimized artificial neural network for modeling axial capacity of pile foundations. *Engineering with Computers*, 37(1), 675-684. https://doi.org/10.1007/s00366-019-00847-5.

Boadu, F.K., Owusu-Nimo, F., Achampong, F., & Ampadu, S.I.K. (2013). Artificial neural network and statistical models for predicting the basic geotechnical properties of soils from electrical measurements. *Near Surface Geophysics*, 11(6), 599-612. https://doi.org/10.3997/1873-0604.2013011.

Camelo, C.S., Lopera, J.F.B., & Perez, J.A.R. (2017). Projeto de estabilização de encostas: caso de estudo San António de Prado – Colômbia. In *Anais do 12ª Conferência Brasileira sobre Estabilidade de Encostas*. Florianópolis. ABMS (in Portuguese).

Carvalho, D. (1991). *Análise de cargas últimas à tração de estacas escavadas, instrumentadas, em campo experimental de São Carlos – SP* [Doctoral thesis]. University of São Paulo (in Portuguese).

Chala, A.T., & Ray, R. (2023a). Assessing the performance of machine learning algorithms for soil classification using cone penetration test data. *Applied Sciences (Basel, Switzerland)*, 13(9), 5758. https://doi.org/10.3390/app13095758.

Chala, A.T., & Ray, R.P. (2023b). Machine learning techniques for soil characterization using cone penetration test data. *Applied Sciences (Basel, Switzerland)*, 13(14), 8286. https://doi.org/10.3390/app13148286.

Cheng, H., Zhang, H., Liu, Z., & Wu, Y. (2023). Prediction of undrained bearing capacity of skirted foundation in spatially variable soils based on convolutional neural network. *Applied Sciences (Basel, Switzerland)*, 13(11), 6624. https://doi.org/10.3390/app13116624.

Coutinho, R.Q., Souza Neto, J.B., & Costa, F.Q. (2000). Design strength parameters of a slope on unsaturated gneissic residual soil. In *Proceedings of Sessions of Geo-Denver 2000 - Advances in Unsaturated Geotechnics* (pp. 247-261). ASCE. https://doi.org/10.1061/40510(287)17.

Dantas Neto, S.A., Silveira, M.V., Amâncio, L.B., & Anjos, G.J.M. (2014). Pile settlement modeling with multilayer perceptrons. *The Electronic Journal of Geotechnical Engineering*, 19, 4517-4528.

Dantas Neto, S.A., Indraratna, B., Oliveira, D.A.F., & Assis, A.P. (2017). Modelling the shear behaviour of clean rock discontinuities using artificial neural networks. *Rock Mechanics and Rock Engineering*, 50(7), 1817-1831. https://doi.org/10.1007/s00603-017-1197-z.

Dias, R.D. (1987). *Aplicação de pedologia e geotecnia no projeto de fundações de linhas de transmissão* [Doctoral thesis]. Federal University of Rio de Janeiro (in Portuguese).

Díaz, E., Brotons, V., & Tomás, R. (2018). Use of artificial neural networks to predict 3-D elastic settlement of foundations on soils with inclined bedrock. *Soil and Foundation*, 58(6), 1414-1422. https://doi.org/10.1016/j.sandf.2018.08.001.

Dolatshahi, A., & Molladavoodi, H. (2024). Prediction of rock tensile fracture toughness: hybrid ANN-WOA Model Approach. *Rudarsko-geološko-Naftni Zbornik*, 39(3), 1-12. https://doi.org/10.17794/rgn.2024.3.1.

Dowlatshahi, M.B., Hashemi, A., Samaei, M. & Momeni, E. (2023). Feasibility of artificial intelligence techniques in rock characterization. In E. Momeni, D. Jahed Armaghani, & A. Azizi (Eds.), *Artificial intelligence in mechatronics and civil engineering* (pp. 93-110). Springer. https://doi.org/10.1007/978-981-19-8790-8_4.

Elsawy, M.B.D., Alsharekh, M.F., & Shaban, M. (2022). Modeling undrained shear strength of sensitive alluvial soft clay using a machine learning approach. *Applied Sciences (Basel, Switzerland)*, 12(19), 10177. https://doi.org/10.3390/app121910177.

Gajan, S. (2023). Prediction of acceleration amplification ratio of rocking foundations using machine learning and deep learning models. *Applied Sciences (Basel, Switzerland)*, 13(23), 12791. https://doi.org/10.3390/app132312791.

Gao, W., Ge, S., Gao, Y., & Yuan, S. (2024). Prediction of utility tunnel performance in a soft foundation during an operation period based on deep learning. *Applied Sciences (Basel, Switzerland)*, 14(6), 2334. https://doi.org/10.3390/app14062334.

Gomes, C.L.R. (2003). *Retroanálise em estabilidade de taludes em solo: metodologia para obtenção dos parâmetros de resistência ao cisalhamento* [Master's dissertation]. State University of Campinas (in Portuguese).

Gon, F.S. (2011). *Caracterização geotécnica através de ensaios de laboratório de um solo de diabásio da região de Campinas/SP* [Master's dissertation]. State University of Campinas (in Portuguese).

Goudjil, K., & Arabet, L. (2021). Assessment of deflection of pile implanted on slope by artificial neural network. *Neural Computing & Applications*, 33(4), 1091-1101. https://doi.org/10.1007/s00521-020-04985-6.

Gupta, A., Aggarwal, Y., & Aggarwal, P. (2022). Deep neural network and ANN ensemble for slope stability prediction. *Archives of Materials Science and Engineering*, 116(1), 14-27. https://doi.org/10.5604/01.3001.0016.0975.

Haykin, S. (2009). *Neural networks: a comprehensive foundation* (3rd ed.). Upper Saddle River, NJ: Pearson Education.

Iyeke, S., Eze, E., Ehiorobo, J., & Osuji, S. (2016). Estimation of shear strength parameters of lateritic soils using artificial neural network. *Nigerian Journal of Technology*, 35(2), 260. https://doi.org/10.4314/njt.v35i2.5.

Janiesch, C., Zschech, P., & Heinrich, K. (2021). Machine learning and deep learning. *Electronic Markets*, 31(3), 685-695. https://doi.org/10.1007/s12525-021-00475-2.

Khatti, J., & Grover, D.K.S. (2022). Determination of suitable hyperparameters of artificial neural network for the best prediction of geotechnical properties of soil. *International Journal for Research in Applied Science and Engineering Technology*, 10(5), 4934-4961. https://doi.org/10.22214/ijraset.2022.43662.

Labuz, J.F., & Zang, A. (2012). Mohr-Coulomb failure criterion. *Rock Mechanics and Rock Engineering*, 45(6), 975-979. https://doi.org/10.1007/s00603-012-0281-7.

Lafayette, K.P.V. (2006). *Estudo geológico-geotécnico do processo erosivo em encostas no parque metropolitano Armando de Holanda Cavalcanti - Cabo de Santo Agostinha/PE* [Master's dissertation]. Federal University of Pernambuco (in Portuguese).

Lambe, T.W., & Whitman, R.V. (1979). *Soil Mechanics, SI version*. John Wiley & Sons.

Lee, S., Kang, J., & Kim, J. (2023). Prediction modeling of ground subsidence risk based on machine learning using the attribute information of underground utilities in urban areas in Korea. *Applied Sciences (Basel, Switzerland)*, 13(9), 5566. https://doi.org/10.3390/app13095566.

Lendo-Siwicka, M., Zabłocka, K., Soból, E., Markiewicz, A., & Wrzesiński, G. (2023). Application of an artificial neural network (ANN) model to determine the value of the damping ratio (D) of clay soils. *Applied Sciences (Basel, Switzerland)*, 13(10), 6224. https://doi.org/10.3390/app13106224.

Li, C., & Dias, D. (2023). Assessment of the rock elasticity modulus using four hybrid RF models: A combination of data-driven and soft techniques. *Applied Sciences (Basel, Switzerland)*, 13(4), 2373. https://doi.org/10.3390/app13042373.

Lima, A.F. (2002). *Comportamento geomecânico e análise de estabilidade de uma encosta da formação barreiras na área urbana da cidade do Recife* [Master's dissertation]. Federal University of Pernambuco (in Portuguese).

Lin, P., Chen, X., Jiang, M., Song, X., Xu, M., & Huang, S. (2022). Mapping shear strength and compressibility of soft soils with artificial neural networks. *Engineering Geology*, 300, 106585. https://doi.org/10.1016/j.enggeo.2022.106585.

Liu, L., Moayedi, H., Rashid, A.S.A., Rahman, S.S.A., & Nguyen, H. (2020). Optimizing an ANN model with genetic algorithm (GA) predicting load-settlement behaviors of eco-friendly raft-pile foundation (ERP) system. *Engineering with Computers*, 36(1), 421-433. https://doi.org/10.1007/s00366-019-00767-4.

Magalhães, J.S.L.A. (2013). *Estudo de estabilidade da encosta alto do Padre Cícero no município de Camaragibe-PE* [Master's dissertation]. Federal University of Pernambuco (in Portuguese).

Marques, R.F. (2006). *Estudo da capacidade de carga de estacas escavadas com bulbos, executadas em solo não saturado da formação barreiras da cidade de Maceió - AL* [Master's dissertation]. Federal University of Pernambuco (in Portuguese).

McCulloch, W.S., & Pitts, W. (1943). A logical calculus of the ideas immanent in nervous activity. *The Bulletin of Mathematical Biophysics*, 5(4), 115-133. https://doi.org/10.1007/BF02478259.

Meng, J., Mattsson, H., & Laue, J. (2021). Three-dimensional slope stability predictions using artificial neural networks. *International Journal for Numerical and Analytical Methods in Geomechanics*, 45(13), 1988-2000. https://doi.org/10.1002/nag.3252.

Millán, M.A., Galindo, R., & Alencar, A. (2021). Application of artificial neural networks for predicting the bearing capacity of shallow foundations on rock masses. *Rock Mechanics and Rock Engineering*, 54(9), 5071-5094. https://doi.org/10.1007/s00603-021-02549-1.

Moayedi, H., & Hayati, S. (2018). Applicability of a CPT-based neural network solution in predicting load-settlement responses of bored pile. *International Journal of Geomechanics*, 18(6), 06018009. https://doi.org/10.1061/(ASCE)GM.1943-5622.0001125.

Moayedi, H., Mosallanezhad, M., Rashid, A.S.A., Jusoh, W.A.W., & Muazu, M.A. (2020). A systematic review and meta-analysis of artificial neural network application in geotechnical engineering: theory and applications. *Neural Computing & Applications*, 32(2), 495-518. https://doi.org/10.1007/s00521-019-04109-9.

Mohammadi, M., Fatemi Magda, S.M., Talkhablou, M., & Cheshomi, A. (2022). Prediction of the shear strength parameters from easily-available soil properties by means of multivariate regression and artificial neural network methods. *Geomechanics and Geoengineering*, 17(2), 442-454. https://doi.org/10.1080/17486025.2020.1778194.

Moraes, L.S. (2010). *Estacas escavadas com base injetada* [Doctoral thesis]. University of São Paulo (in Portuguese).

Nejad, F.P., & Jaksa, M.B. (2017). Load-settlement behavior modeling of single piles using artificial neural networks and CPT data. *Computers and Geotechnics*, 89, 9-21. https://doi.org/10.1016/j.compgeo.2017.04.003.

Paliwal, M., Goswami, H., Ray, A., Bharati, A. K., Rai, R., & Khandelwal, M. (2022). Stability prediction of residual soil and rock slope using artificial neural network. *Advances in Civil Engineering*, 2022(1), 4121193. https://doi.org/10.1155/2022/4121193.

Parhi, R., & Nowak, R.D. (2020). The role of neural network activation functions. *IEEE Signal Processing Letters*, 27, 1779-1783. https://doi.org/10.1109/LSP.2020.3027517.

Peixoto, A.S.P. (2001). *Estudo do ensaio SPT-T e sua aplicação na prática da engenharia de fundações* [Doctoral thesis]. State University of Campinas (in Portuguese).

Pérez, N.B.M. (2014). *Análise de transferência de carga em estacas escavadas em solo da região de Campinas/SP* [Master's dissertation]. State University of Campinas (in Portuguese).

Ray, R., Kumar, D., Samui, P., Roy, L.B., Goh, A.T.C., & Zhang, W. (2021). Application of soft computing techniques for shallow foundation reliability in geotechnical engineering. *Geoscience Frontiers*, 12(1), 375-383. https://doi.org/10.1016/j.gsf.2020.05.003.

Ribeiro, V., Villar, L., Mendonça, A., & Caldas, M. (2012). Análise de uma contenção em retangulões instrumentada. In *Anais do 16º Congresso Brasileiro de Mecânica dos Solos e Engenharia Geotécnica*. Porto de Galinhas. ABMS (in Portuguese).

Rumelhart, D.E., Hinton, G.E., & Williams, R.J. (1986). Learning representations by back-propagating errors. *Nature*, 323, 533-536. https://doi.org/10.1038/323533a0.

Santana, L.G. (2016). Estimativa de parâmetros de resistência ao cisalhamento de solos a partir de sondagens SPT e comparação com resultados de ensaios triaxiais. In *Anais do 18º Congresso Brasileiro de Mecânica dos Solos e Engenharia Geotécnica*. Belo Horizonte. ABMS (in Portuguese). https://doi.org/10.20906/CPS/CB-01-0174.

Santos, M.A.A. (2007). *Influência das condições tridimensionais de tensão e fluxo na estabilidade de um talude em solo não saturado* [Master's dissertation]. University of Brasília (in Portuguese).

Schmertmann, J.H., & Palacios, A. (1979). Energy dynamics of SPT. *Journal of the Geotechnical Engineering Division*, 105(8), 909-926. https://doi.org/10.1061/AJGEB6.0000839.

Sethy, B.P., Patra, C., Das, B.M., & Sobhan, K. (2021). Prediction of ultimate bearing capacity of circular foundation on sand layer of limited thickness using artificial neural network. *International Journal of Geotechnical Engineering*, 15(10), 1252-1267. https://doi.org/10.1080/19386362.2019.1645437.

Silva, M.M. (2007). *Estudo geológico-geotécnico de uma encosta com problemas de instabilidade no município de Camaragibe-PE* [Doctoral thesis]. Federal University of Pernambuco (in Portuguese).

Souza, A.P.L. (2014). *Estudos geotécnicos e de estabilidade de taludes da encosta do Alto do padre Cícero no município de Camaragibe-PE* [Master's dissertation]. Federal University of Pernambuco (in Portuguese).

Souza, J.M. (2012). *Abordagem qualitativa e quantitativa de encostas urbanas aplicada a dois taludes no município de Vitória* [Master's dissertation]. Federal University of Ouro Preto (in Portuguese).

Suzuki, S. (2004). *Propriedades geomecânicas de alguns solos residuais e coluviais ao longo do oleoduto Curitiba-Paranaguá* [Master's dissertation]. Federal University of Rio de Janeiro (in Portuguese).

Tizpa, P., Jamshidi, C.R., Karimpour, F.M., & Lemos, M.S. (2015). ANN prediction of some geotechnical properties of soil from their index parameters. *Arabian Journal of Geosciences*, 8(5), 2911-2920. https://doi.org/10.1007/s12517-014-1304-3.

Xiang, X., & Zi-Hang, D. (2017). Numerical implementation of a modified Mohr–Coulomb model and its application in slope stability analysis. *Journal of Modern Transportation*, 25(1), 40-51. https://doi.org/10.1007/s40534-017-0123-0.

Yang, T., Wen, T., Huang, X., Liu, B., Shi, H., Liu, S., Peng, X., & Sheng, G. (2024). Predicting model of dual-mode shield tunneling parameters in complex ground using recurrent neural networks and multiple optimization algorithms. *Applied Sciences (Basel, Switzerland)*, 14(2), 581. https://doi.org/10.3390/app14020581.

Zhan, T., Guo, X., Jiang, T., & Jiang, A. (2023). Intelligent feedback analysis of fluid–solid coupling of surrounding rock of tunnel in water-rich areas. *Applied Sciences (Basel, Switzerland)*, 13(3), 1479. https://doi.org/10.3390/app13031479.

Zhang, C., Bengio, S., Hardt, M., Recht, B., & Vinyals, O. (2021). Understanding deep learning (still) requires rethinking generalization. *Communications of the ACM*, 64(3), 107-115. https://doi.org/10.1145/3446776.

Zhang, P., Yin, Z.Y., & Jin, Y.F. (2022). Bayesian neural network-based uncertainty modelling: application to soil compressibility and undrained shear strength prediction. *Canadian Geotechnical Journal*, 59(4), 546-557. https://doi.org/10.1139/cgj-2020-0751.

Zheng, F., Jiang, A., Guo, X., Min, Q., & Yin, Q. (2022). Back analysis of surrounding rock parameters of large-span arch cover station based on GP-DE algorithm. *Applied Sciences (Basel, Switzerland)*, 12(24), 12590. https://doi.org/10.3390/app122412590.

Appendix A. Training and test database.

Table A1. Training and test database.

Depth (m)	NSPT	σ'v (kPa)	c' (kPa)	ϕ' (º)	Soil type	Group	Test type	Reference
3.00	14.00	50.03	30.00	34.00	clayey sand	sandy	Triaxial	Santana (2016)
1.50	2.00	25.95	47.00	44.20	clayey sand	sandy	Direct shear	Silva (2007)
4.30	5.00	74.38	4.40	38.90	clayey sand	sandy	Direct shear	Silva (2007)
4.90	10.00	84.76	3.80	31.50	clayey sand	sandy	Direct shear	Silva (2007)
1.50	3.00	24.90	3.70	31.20	clayey sand	sandy	Direct shear	Silva (2007)
1.50	3.00	24.90	45.70	31.30	clayey sand	sandy	Direct shear	Silva (2007)
5.70	19.00	94.62	6.30	40.40	clayey sand	sandy	Direct shear	Silva (2007)
6.30	18.00	104.58	2.20	35.00	sandy clay	clayey	Direct shear	Silva (2007)
1.50	7.00	26.25	3.80	29.40	clayey sand	sandy	Direct shear	Silva (2007)
1.50	7.00	26.25	42.30	43.70	clayey sand	sandy	Direct shear	Silva (2007)
2.50	6.00	41.50	9.70	26.30	sandy clay	clayey	Direct shear	Silva (2007)
2.50	6.00	41.50	9.80	29.20	sandy clay	clayey	Direct shear	Silva (2007)
6.00	11.00	99.60	3.00	27.60	sandy clay	clayey	Direct shear	Silva (2007)
2.00	5.00	33.83	27.39	35.70	sandy clay	clayey	Direct shear	Magalhães (2013)
2.00	5.00	33.85	8.72	34.20	sandy clay	clayey	Direct shear	Magalhães (2013)
2.00	4.00	36.12	35.08	28.10	sandy clay	clayey	Direct shear	Magalhães (2013)
2.00	4.00	36.09	6.97	29.50	sandy clay	clayey	Direct shear	Magalhães (2013)
2.00	4.00	32.45	13.76	36.50	clayey sand	sandy	Direct shear	Magalhães (2013)
2.00	4.00	32.68	3.30	35.10	clayey sand	sandy	Direct shear	Magalhães (2013)
1.50	6.00	22.50	10.00	35.00	clayey sand	sandy	Direct shear	Souza (2014)
1.50	6.00	27.75	1.00	32.00	clayey sand	sandy	Direct shear	Souza (2014)
1.50	5.00	24.45	7.02	35.32	sandy clay	clayey	Direct shear	Souza (2014)
1.50	5.00	29.25	2.85	31.62	sandy clay	clayey	Direct shear	Souza (2014)
1.50	11.00	27.30	28.75	32.92	sandy clay	clayey	Direct shear	Souza (2014)
1.50	11.00	30.45	6.19	30.73	sandy clay	clayey	Direct shear	Souza (2014)
0.75	4.00	12.75	71.40	41.60	clayey sand	sandy	Direct shear	Coutinho et al. (2000)
0.75	4.00	12.75	10.80	31.90	clayey sand	sandy	Direct shear	Coutinho et al. (2000)
8.70	20.00	147.90	7.00	29.50	sandy silt	silty	Direct shear	Coutinho et al. (2000)
8.70	20.00	147.90	5.30	31.40	sandy silt	silty	Direct shear	Coutinho et al. (2000)
1.04	2.00	18.14	28.00	31.00	clayey sand	sandy	Direct shear	Lima (2002)
1.04	2.00	18.88	10.00	32.00	clayey sand	sandy	Direct shear	Lima (2002)
1.10	13.00	25.21	84.00	34.00	silty sand	sandy	Direct shear	Lima (2002)
1.10	13.00	23.80	1.00	16.00	silty sand	sandy	Direct shear	Lima (2002)
1.00	3.00	17.41	10.00	31.60	clayey silt	silty	Direct shear	Suzuki (2004)
3.50	14.00	62.22	8.00	33.00	clayey silt	silty	Direct shear	Suzuki (2004)
3.50	5.00	61.77	11.00	31.50	sandy silt	silty	Direct shear	Suzuki (2004)
2.40	2.00	29.52	20.00	29.00	clayey sand	sandy	Direct shear	Santos (2007)
2.40	2.00	29.52	3.00	27.00	clayey sand	sandy	Direct shear	Santos (2007)
5.00	6.00	71.00	20.00	27.00	clayey sand	sandy	Direct shear	Santos (2007)
5.00	6.00	71.00	4.70	27.00	clayey sand	sandy	Direct shear	Santos (2007)
7.70	11.00	117.04	27.00	36.00	clayey sand	sandy	Direct shear	Santos (2007)
7.70	11.00	117.04	4.20	30.00	clayey sand	sandy	Direct shear	Santos (2007)
11.70	5.00	184.86	35.00	31.00	clayey sand	sandy	Direct shear	Santos (2007)
11.70	5.00	184.86	14.00	30.00	clayey sand	sandy	Direct shear	Santos (2007)
1.10	5.00	16.23	9.76	31.20	sandy silt	silty	Direct shear	Marques (2006)
1.10	5.00	16.23	0.00	31.90	sandy silt	silty	Direct shear	Marques (2006)
3.10	4.00	47.59	15.75	27.20	sandy silt	silty	Direct shear	Marques (2006)
3.10	4.00	47.59	0.00	30.00	sandy silt	silty	Direct shear	Marques (2006)
5.10	8.00	92.51	17.18	31.60	sandy silt	silty	Direct shear	Marques (2006)
5.10	8.00	92.51	0.00	31.80	sandy silt	silty	Direct shear	Marques (2006)
7.20	16.00	132.19	7.25	32.70	silty sand	sandy	Direct shear	Marques (2006)

Table A1. Continued...

Depth (m)	NSPT	σ’v (kPa)	c’ (kPa)	ϕ’ (º)	Soil type	Group	Test type	Reference
7.20	16.00	132.19	0.00	34.90	silty sand	sandy	Direct shear	Marques (2006)
8.40	19.00	150.61	21.65	36.10	silty sand	sandy	Direct shear	Marques (2006)
8.40	19.00	150.61	1.64	27.90	silty sand	sandy	Direct shear	Marques (2006)
2.44	4.00	47.53	6.31	28.37	silty sand	sandy	Direct shear	Souza (2012)
2.44	4.00	47.53	59.05	43.23	silty sand	sandy	Direct shear	Souza (2012)
4.70	22.00	85.16	8.05	30.11	silty sand	sandy	Direct shear	Souza (2012)
4.70	22.00	85.16	93.49	41.99	silty sand	sandy	Direct shear	Souza (2012)
2.44	4.00	47.53	4.80	24.70	silty sand	sandy	Triaxial	Souza (2012)
4.70	22.00	85.16	12.36	23.75	silty sand	sandy	Triaxial	Souza (2012)
1.02	10.00	17.87	94.45	54.46	silty sand	sandy	Direct shear	Souza (2012)
1.02	10.00	17.87	13.50	26.96	silty sand	sandy	Direct shear	Souza (2012)
1.37	10.00	24.00	7.40	39.69	silty sand	sandy	Direct shear	Souza (2012)
1.37	10.00	24.00	2.72	37.15	silty sand	sandy	Direct shear	Souza (2012)
1.02	10.00	17.87	9.17	24.23	silty sand	sandy	Triaxial	Souza (2012)
1.37	10.00	24.00	0.00	27.02	silty sand	sandy	Triaxial	Souza (2012)
1.50	2.00	24.00	0.00	35.00	silty sand	sandy	Triaxial	Gomes (2003)
1.50	2.00	24.00	11.00	22.30	silty sand	sandy	Triaxial	Gomes (2003)
1.50	15.00	27.00	37.20	25.70	clayey sand	sandy	Triaxial	Gomes (2003)
1.50	15.00	27.00	68.90	24.10	clayey sand	sandy	Triaxial	Gomes (2003)
1.80	24.00	28.96	33.10	33.40	silty sand	sandy	Direct shear	Lafayette (2006)
1.80	24.00	28.96	1.60	33.80	silty sand	sandy	Direct shear	Lafayette (2006)
4.80	25.00	74.40	43.70	41.30	silty sand	sandy	Direct shear	Lafayette (2006)
4.80	25.00	74.40	8.20	30.30	silty sand	sandy	Direct shear	Lafayette (2006)
1.80	30.00	26.24	56.10	35.70	silty sand	sandy	Direct shear	Lafayette (2006)
1.80	30.00	26.24	1.80	35.00	silty sand	sandy	Direct shear	Lafayette (2006)
12.30	28.00	196.19	45.60	41.00	silty sand	sandy	Direct shear	Lafayette (2006)
12.30	28.00	196.19	7.60	31.30	silty sand	sandy	Direct shear	Lafayette (2006)
0.50	7.00	8.85	23.00	31.00	sandy clay	clayey	Direct shear	Dias (1987)
0.50	7.00	8.80	14.00	26.00	sandy clay	clayey	Direct shear	Dias (1987)
1.50	7.00	24.60	32.00	26.00	sandy clay	clayey	Direct shear	Dias (1987)
1.50	7.00	24.45	16.00	24.00	sandy clay	clayey	Direct shear	Dias (1987)
0.50	11.00	8.85	54.60	30.50	sandy clay	clayey	Direct shear	Dias (1987)
0.50	11.00	8.40	32.00	27.90	sandy clay	clayey	Direct shear	Dias (1987)
1.50	10.00	24.30	39.00	38.60	sandy clay	clayey	Direct shear	Dias (1987)
1.50	10.00	24.15	31.00	33.50	sandy clay	clayey	Direct shear	Dias (1987)
0.50	40.00	8.55	41.50	35.60	sandy clay	clayey	Direct shear	Dias (1987)
0.50	40.00	8.15	25.00	28.70	sandy clay	clayey	Direct shear	Dias (1987)
7.00	10.00	160.30	0.00	37.00	sand	sandy	Direct shear	AbdelSalam et al. (2014)
13.70	28.00	345.24	0.00	39.00	sand	sandy	Direct shear	AbdelSalam et al. (2014)
2.10	26.00	42.42	7.20	37.00	sand with gravel	sandy	Direct shear	Abdelsalam et al. (2014)
7.60	40.00	182.40	32.20	29.00	sand with gravel	sandy	Direct shear	AbdelSalam et al. (2014)
13.70	24.00	324.69	0.20	41.00	sand with gravel	sandy	Direct shear	AbdelSalam et al. (2014)
1.00	25.00	20.20	0.00	28.00	clayey sand	sandy	Direct shear	AbdelSalam et al. (2014)
3.50	45.00	84.00	10.00	32.00	clayey sand	sandy	Direct shear	Abdelsalam et al. (2014)
11.50	90.00	272.55	40.00	35.00	clayey sand	sandy	Direct shear	AbdelSalam et al. (2014)
4.00	30.00	80.00	35.60	24.00	silty sand	sandy	Direct shear	Ribeiro et al. (2012)
4.00	30.00	80.00	112.30	30.10	silty sand	sandy	Direct shear	Ribeiro et al. (2012)
1.00	18.00	17.00	8.00	15.00	clayey silt	silty	Direct shear	Camelo et al. (2017)
6.00	35.00	96.00	10.00	26.00	clayey silt	silty	Direct shear	Camelo et al. (2017)
13.00	45.00	208.00	17.00	21.00	clayey silt	silty	Direct shear	Camelo et al. (2017)
22.00	12.00	401.72	37.70	17.00	clayey silt	silty	Direct shear	Camelo et al. (2017)
1.00	10.00	20.00	20.00	25.00	silt	silty	Direct shear	Camelo et al. (2017)
5.00	15.00	95.00	20.00	23.00	silt	silty	Direct shear	Camelo et al. (2017)

Table A1. Continued...

Depth (m)	NSPT	σ’v (kPa)	c’ (kPa)	ϕ’ (º)	Soil type	Group	Test type	Reference
10.00	20.00	200.00	24.00	27.00	silt	silty	Direct shear	Camelo et al. (2017)
15.00	20.00	270.00	24.00	28.00	silt	silty	Direct shear	Camelo et al. (2017)
1.00	5.00	19.00	11.00	28.00	silty sand	sandy	Direct shear	Camelo et al. (2017)
6.00	8.00	114.00	8.00	30.00	silty sand	sandy	Direct shear	Camelo et al. (2017)
10.00	20.00	180.00	20.00	25.00	silt	silty	Direct shear	Camelo et al. (2017)
14.00	30.00	252.00	15.00	28.00	silt	silty	Direct shear	Camelo et al. (2017)
20.00	25.00	420.00	20.00	28.00	silty sand	sandy	Direct shear	Camelo et al. (2017)
1.50	2.00	21.95	0.00	33.40	silty sand	sandy	Direct shear	Camelo et al. (2017)
1.50	2.00	21.93	0.00	32.50	silty sand	sandy	Direct shear	Camelo et al. (2017)
1.50	5.00	22.01	0.00	31.30	silty sand	sandy	Direct shear	Camelo et al. (2017)
3.00	4.00	43.29	4.00	27.70	silty sand	sandy	Direct shear	Carvalho (1991)
15.00	26.00	306.01	0.00	36.50	silty sand	sandy	Direct shear	Carvalho (1991)
4.50	2.00	98.18	3.00	16.20	clayey sand	sandy	Triaxial	Carvalho (1991)
9.00	42.00	17.85	46.00	5.31	clayey sand	sandy	Triaxial	Carvalho (1991)
1.30	5.00	20.00	6.00	30.50	clayey sand	sandy	Triaxial	Carvalho (1991)
2.30	2.00	35.40	5.00	29.50	clayey sand	sandy	Triaxial	Carvalho (1991)
3.30	3.00	50.80	6.00	30.00	clayey sand	sandy	Triaxial	Carvalho (1991)
4.30	4.00	67.40	12.50	29.00	clayey sand	sandy	Triaxial	Carvalho (1991)
5.30	5.00	84.70	1.00	31.00	clayey sand	sandy	Triaxial	Carvalho (1991)
6.30	3.00	102.10	25.50	25.00	clayey sand	sandy	Triaxial	Carvalho (1991)
7.30	7.00	120.70	4.50	28.00	clayey sand	sandy	Triaxial	Carvalho (1991)
8.30	7.00	139.20	18.00	23.00	clayey sand	sandy	Triaxial	Carvalho (1991)
9.30	9.00	157.00	9.00	26.00	clayey sand	sandy	Triaxial	Carvalho (1991)
10.30	7.00	176.00	43.00	14.00	clayey sand	sandy	Triaxial	Carvalho (1991)
1.50	2.10	15.00	0.00	32.00	clayey sand	sandy	Triaxial	Peixoto (2001)
2.50	0.60	30.00	14.00	31.00	clayey sand	sandy	Triaxial	Peixoto (2001)
3.50	1.50	46.00	22.00	20.00	clayey sand	sandy	Triaxial	Peixoto (2001)
4.50	1.50	62.00	24.00	28.00	clayey sand	sandy	Triaxial	Peixoto (2001)
5.50	1.50	78.00	14.00	29.00	clayey sand	sandy	Triaxial	Peixoto (2001)
7.50	4.10	94.00	20.00	29.00	clayey sand	sandy	Triaxial	Peixoto (2001)
7.50	4.10	110.00	0.00	32.00	clayey sand	sandy	Triaxial	Peixoto (2001)
8.50	5.50	126.00	35.00	28.00	clayey sand	sandy	Triaxial	Peixoto (2001)
10.50	6.60	142.00	16.00	30.00	clayey sand	sandy	Triaxial	Peixoto (2001)
10.50	6.60	158.00	14.00	29.00	clayey sand	sandy	Triaxial	Peixoto (2001)
12.50	7.70	174.00	49.00	25.00	clayey sand	sandy	Triaxial	Peixoto (2001)
12.50	7.70	190.00	26.00	29.00	clayey sand	sandy	Triaxial	Peixoto (2001)
1.00	4.92	16.00	0.00	32.20	clayey sand	sandy	Triaxial	Peixoto (2001)
2.00	2.55	30.80	3.00	31.80	clayey sand	sandy	Triaxial	Peixoto (2001)
3.00	2.70	45.70	2.00	32.50	clayey sand	sandy	Triaxial	Peixoto (2001)
5.00	3.92	75.30	2.00	33.30	clayey sand	sandy	Triaxial	Peixoto (2001)
7.00	4.48	107.10	3.00	33.00	clayey sand	sandy	Triaxial	Peixoto (2001)
9.00	6.88	143.90	16.00	30.30	clayey sand	sandy	Triaxial	Peixoto (2001)
11.00	8.38	179.30	20.00	28.80	clayey sand	sandy	Triaxial	Peixoto (2001)
13.00	8.43	216.90	20.00	28.80	clayey sand	sandy	Triaxial	Peixoto (2001)
15.00	10.33	250.90	17.00	30.10	clayey sand	sandy	Triaxial	Peixoto (2001)
3.00	2.00	45.00	0.00	29.03	clayey sand	sandy	Triaxial	Moraes (2010)
5.00	3.00	75.00	10.50	31.20	clayey sand	sandy	Triaxial	Moraes (2010)
8.00	6.00	111.00	26.90	26.40	clayey sand	sandy	Triaxial	Moraes (2010)
1.00	2.00	14.10	7.40	22.00	clayey sand	sandy	Triaxial	Pérez (2014)
2.00	4.00	28.20	7.90	21.00	Silty clay	clayey	Triaxial	Pérez (2014)
3.00	4.00	42.20	11.60	22.00	Silty clay	clayey	Triaxial	Pérez (2014)
4.00	5.00	56.60	5.80	23.00	Silty clay	clayey	Triaxial	Pérez (2014)
5.00	7.00	72.10	24.00	21.00	Silty clay	clayey	Triaxial	Pérez (2014)

Table A1. Continued...

Depth (m)	NSPT	σ'v (kPa)	c' (kPa)	ϕ' (º)	Soil type	Group	Test type	Reference
6.00	7.00	87.40	42.40	22.00	Silty clay	clayey	Triaxial	Pérez (2014)
7.00	7.00	102.80	41.90	22.00	Silty clay	clayey	Triaxial	Pérez (2014)
8.00	7.00	118.00	26.40	22.00	Silty clay	clayey	Triaxial	Pérez (2014)
1.00	2.00	10.96	7.40	22.00	Clayey silt	silty	Triaxial	Gon (2011)
2.00	4.00	22.18	7.90	21.00	Silty sand	sandy	Triaxial	Gon (2011)
3.00	2.00	32.70	11.60	22.00	Silty sand	sandy	Triaxial	Gon (2011)
4.00	4.00	46.00	5.80	23.00	Silty sand	sandy	Triaxial	Gon (2011)
5.00	4.00	61.50	24.00	21.00	Silty sand	sandy	Triaxial	Gon (2011)
6.00	7.00	72.30	42.40	22.00	Sandy clay	clayey	Triaxial	Gon (2011)
7.00	7.00	84.00	41.90	22.00	Sandy clay	clayey	Triaxial	Gon (2011)
8.00	7.00	92.00	26.40	22.00	Sandy clay	clayey	Triaxial	Gon (2011)